A low-cost multimodal Biometric Sensor to capture Finger Vein and Fingerprint

R. Raghavendra   Kiran B Raja   Jayachander Surbiryala   Christoph Busch

Norwegian Biometric Laboratory, Gjøvik University College, Norway

Email: raghavendra.ramachandra, kiran.raja, jayachander.surbiryala, christoph.busch@hig.no

Abstract

Multimodal biometric systems based on fingerprint and finger vein modality provide promising features useful for robust and reliable identity verification. In this paper, we present a robust imaging device that can capture both fingerprint and finger vein simultaneously. The presented low-cost sensor employs a single camera followed by both near infrared and visible light sources organized along with the physical structures to capture good quality finger vein and fingerprint samples. We further present a novel finger vein recognition algorithm that explores both the maximum curvature method and Spectral Minutiae Representation (SMR). Extensive experiments are carried out on our newly collected database that comprises of 1500 samples of fingerprint and finger vein from 150 unique fingers corresponding to 41 subjects. Our results demonstrate the efficacy of the proposed sensor with a lowest Equal Error Rate of 0.78%.

1. Introduction

The concept of multimodal biometric system has gained enormous attention because of their reliable and accurate identity verification. Moreover large scale identification systems like the Indian UID system are based on multimodal and also multi-instance biometrics in order to achieve the required accuracy. Among the different biometric modalities that can be used to constitute a multimodal biometric system the use of fingerprint and finger vein appears to be more refined because: (1) The human fingers are highly convenient for imaging and disclose variety of features when captured in different spectrums. For instance, imaging the finger with visible spectrum will disclose the texture features present on the finger surface that in turn can be used to extract minutiae features of the fingerprint or the line features of the whole finger. While imaging the finger with a near infrared spectrum will allow one to capture the

finger vein pattern. (2) Low verification error rates can be achieved by combining these complementary features available from the single biometric modality i.e, finger. (3) Use of finger-vein shows strong anti-spoofing nature as it is hidden inside the finger and cannot be stolen without subject co-operation. (4) The two biometric characteristics can be acquired with one capture device and in principle with a single capture attempt. These factors motivate us to explore a new capture device to reliably observe the prominent information from the finger that in turn can be used to build a multimodal biometric system using fingerprint and finger vein images for robust identity verification.

The multimodal biometric identification using fingerprint and finger vein has witnessed wide interest from both academia and industry. Park et al. [10] introduced a fingerprint and finger vein sensor such that these two biometric modalities are captured independently using two separate dedicated sensors. Here, the optical fingerprint is used to capture fingerprint samples and a camera with near infrared light source is used to capture the finger vein. Finally, Local Binary Pattern (LBP) algorithm is used independently on fingerprint and finger vein to assess the performance of the sensor. Lee et al. [5] introduced a portable fingerprint and finger vein biometric sensor that employs two separate high resolution cameras to capture fingerprint and finger vein separately. The performance of the sensor was evaluated on a very small database using minutiae based feature extraction and modified Hausdorff distance on both fingerprint and finger vein independently. Kumar et al. [4] introduced the sensor to capture the finger vein and finger surface. Here, the normal camera is used to capture the finger surface that can reflect the texture features corresponding to the line patterns. In addition to this, another near infrared camera is used to capture the finger vein pattern of the finger. Finally, the performance of the sensor is measured with various feature extraction techniques employed independently on fingerprint and finger-vein that in turn fused at comparison score level. Apart from the academic research, Morpho has introduced a set of devices capable of capturing the fingerprint and finger-vein [8].

In this work, we present a new fingerprint and finger vein

sensor that can simultaneously capture both of these biometric characteristics. Unlike the state-of-the-art schemes that employed two separate sensors which can independently capture both fingerprint and finger vein, our proposed device is tailored to use a single camera to capture both in a contact less fashion. Further, we have also designed the light sources (for both near infrared and visible light) with supporting physical structures to get adequate amount of light intensity to achieve good quality imaging of both fingerprint and finger vein. Thus, the developed multimodal biometric capture device offers wide varieties of advantages that include: (1) Low cost (2) Portability (3) Extract prominent information from both fingerprint and finger vein (4) User friendliness. The main contributions of this paper can be summarized as follows: (1) New sensor is presented to simultaneously capture both fingerprint and finger vein biometrics. The developed sensor captures images in a contactless fashion utilizing a peg-free approach and is also user-friendly (2) New multimodal biometric database consisting of 1500 samples that represent 150 unique fingers from 41 subjects are collected using our sensor. In addition, we also provide a companion protocol for benchmarking the performance of the system (3) A new finger vein recognition method is presented based on a maximum curvature algorithm and computing the spectral minutiae representation of the finger vein pattern. (4) Extensive experiments are carried out on our database, which consistently show the superiority of the proposed finger vein recognition approach when compared against four different well adopted state-of-the-art schemes [7, 2, 6, 4]. Further, the performance achieved using weighted comparison score level fusion of fingerprint and finger vein shows the applicability of the proposed sensor for real-life scenario.

The rest of the paper is organized as follows: Section 2 presents the details on the multimodal capture device designed to capture fingerprint and finger vein. Section 3 presents the details on our data base construction and companion protocols. Section 4 describes the complete pipeline adopted in the proposed multimodal scheme for robust identity verification using fingerprint and finger vein. Section 5 presents the obtained results and comparative analysis of the proposed finger vein recognition with state-of-the-art schemes and finally, Section 6 draws the conclusion.

2. Fingerprint and finger vein acquisition setup

This section will present the details of our custom transillumination device designed to capture both fingerprint and finger vein biometric characteristics. The main objective of our design is to capture three fingers of the hand - index, middle and ring finger. The other two fingers are not included because of their different shape when compared to rest of three fingers. Also, it is more convenient for the subject to use either index, middle or ring finger when com-

pared to thumb and little finger, especially when interacting with our sensor due to compact design. The acquisition device introduced in this work is based on both light penetration (or transmission) method to capture the finger vein and light reflection method to capture the fingerprint image (or photo) from the same finger.
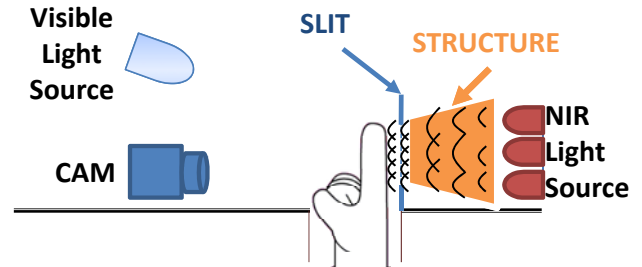

Figure 1. Layout of the fingerprint and finger vein capture device

Figure 1 shows the schematic cross-section of the fingerprint and finger vein capture device introduced in this work. The proposed multimodal biometric capture device consists of four integral units - (1) Near infrared light source (2) Physical structures to achieve the adequate intensity of light (3) Visible light source (4) Camera and lens. Figure 2 (a) shows the infrared light source that consists of a cluster of Light Emitting Diodes (LEDs) that can emit the adequate amount of light to capture the finger vein. In this work, we employed 40 $TSFF$ 5210 near infrared LEDs produced by Vishey semiconductors with a wavelength of 870nm. We adopted $TSFF$ 5210 LEDs by considering its high radiant intensity and view angle that will allow one to couple more power into a finger.
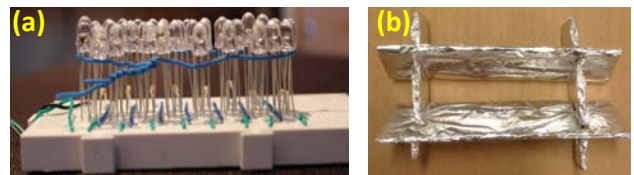

Figure 2. Near infrared lighting components used in our sensor (a) LED source (b) Physical structure to achieve the adequate the light intensity

The crucial part of our capturing device design is to make sure that right amount of light intensity is used to penetrate the finger so that the prominent patterns of the finger vein is successfully captured. In order to achieve this, we propose two different physical structures. The first structure shown in the Figure 2 (b) is used to increase the intensity of the light emitted by LEDs and thereby concentrating all light intensity to the small area. The structure is wrapped with aluminium foil to further achieve high reflectance of the emitted light intensity. In order to equally distribute this intensity of light along the finger we introduce another
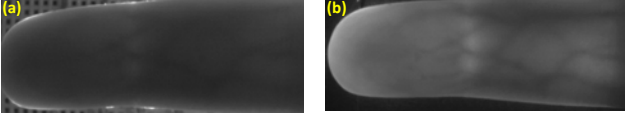
Figure 3. Illustrating the significance of the proposed physical structure to enhance sample quality (a) finger vein image without visible structures (b) finger vein structure with visible structures

physical structure consisting of a slit aligning exactly at the middle of the structure as illustrated in Figure 1 (indicated by blue line). The opening of the slit will distribute the non-uniform light travelling through it to uniform light [1]. Finally, a panel to rest the finger is attached exactly at the position of the slit towards cameras.

The effectiveness of adopting these structures are illustrated in Figure 3. Figure 3 (a) shows the captured image without the use of the proposed physical structures and Figure 3 (b) shows the captured image with physical structures. Here, it can be observed that, the use of the proposed physical structure will significantly improve the quality of the captured finger vein images and thereby justifies the integration of these physical structures.

In this work, we employed the camera DMK 22BUC03 monochrome CMOS camera with a resolution of 744×480 pixel. We particularly select this camera by considering its high quantum efficiency at both visible and near infrared wavelength. The camera has been fitted with a T3Z0312CS lens with a focal length of 8mm. Figure 4 (a) shows the camera with the lens that is employed to construct our sensor.

Figure 4. Components adopted in our sensor (a) camera with lens (b) visible light source

Figure 5 shows the final constructed device to capture the multimodal biometrics. The capture device is portable with a width of 18cms, breadth of 11cms and height of 7cms. Further, additional care is taken by covering both units and the captured finger in a device container to mitigate the effect of external lighting interference. In addition, the user interaction with the sensor is designed such that, the subject can place their fingers irrespective of their size and shape without releasing the pressure on the finger. This is very crucial because of the elastic nature of the finger vein pattern, placement of the finger on the finger rest will result in stretching of the vein patterns due to the released pressure

on the finger. Thus, the user interaction with our sensor is designed at its simplest such that the subject will stretch their finger (either index, middle or ring) towards the designated position so that the imaging of the finger is done in both visible and near infrared wavelength in a sequential manner to capture both fingerprint and finger vein patterns.

Figure 5. Developed fingerprint and finger vein biometric capture device

3. Database Construction

The data collection was carried out at our laboratory in the indoor scenario for the duration of 3 months. The collected dataset consists of 41 subjects whose fingerprint and finger vein images are captured in a single session. Out of 41 subjects, 10 of them are female and rest of them (31 subjects) are male. Among the captured subjects 90% of them belong to the age group of 20-35 years and the remaining were older than this. Each subject presented his index, middle and ring finger of both hands that resulted in 6 different finger instances. However, due to various reason not all subjects have provided all 6 fingers. Each finger image and finger vein were acquired 10 times individually. Thus, the final dataset consists of 1500 samples corresponding to fingerprint and finger vein patterns that represent 150 unique finger instances from 41 subjects. Figure 6 shows sample images of finger vein (Figure 6 (a)) and fingerprint (Figure 6 (b)) captured using our developed multimodal biometric capture device.

3.1. Performance testing protocol

In order to effectively evaluate the performance of the proposed sensor for robust identity verification, we divide the whole database of 150 fingers into two independent subsets, namely: (1) Development dataset (2) Testing dataset. The development dataset consists of 60 fingers that can constitute 600 samples and testing dataset consists of 90 fingers that results in 900 samples. The development dataset is used to tune the pre-processing steps and feature extraction scheme used in this work. While the testing dataset is used solely to report the results. Further both development and testing datasets are further divided into reference and probe samples. Since each finger has 10 samples, we divided 9
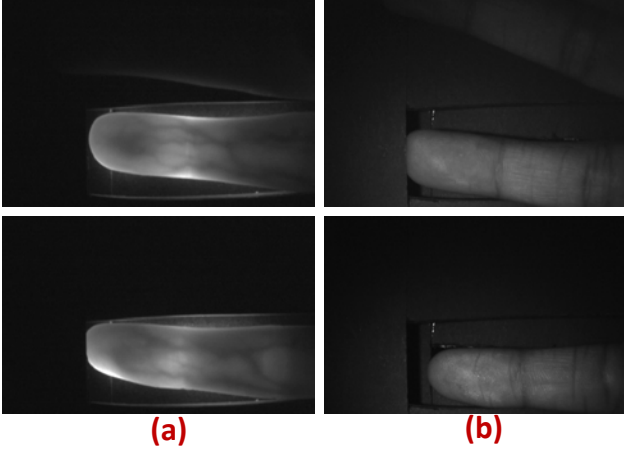
Figure 6. Illustration of the sample images (a) finger vein (b) fingerprint

samples as reference and 1 sample as probe. This partition of reference and probe is repeated using 25 fold leave-one-out cross-validation on the testing dataset to report the final results.
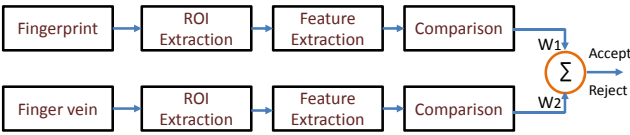
4. Proposed scheme

Figure 7. Block diagram of the proposed verification scheme

Figure 7 shows the block diagram of the proposed scheme for subject verification using the proposed sensor based on fingerprint and finger vein biometrics. Given the fingerprint and finger vein samples, the proposed scheme will perform series of operations that can be considered in four building blocks, namely: (1) Pre-processing and Region-of-Interest (ROI) extraction (2) Feature Extraction (3) Comparison (4) Weighted comparison score level fusion.

4.1. Pre-processing and Region-of-Interest (ROI) extraction of vein images

The pre-processing and ROI extraction steps are carried out independently on finger vein and fingerprint samples. The goal of these steps is to extract the prominent region from the finger by mitigating the background and also to address the alignment by correcting the rotation and translation errors. In the following section, we describe our pre-processing scheme developed for finger vein and fingerprint biometrics.
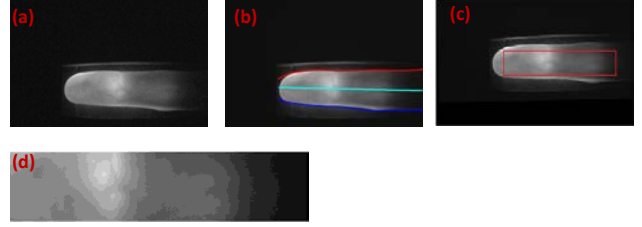

Figure 8. Illustration of finger vein pre-processing and ROI extraction (a) Finger vein sample (b) Boundary extraction (c) Rotation and translation correction (d) ROI Extraction

4.1.1 ROI extraction for finger vein images

The pre-processing step involves in identifying the boundary of the finger region and then compute the axis of the finger as the midpoint between upper and lower boundary of the finger which in turn is used to estimate the translation and rotation error. Figure 8 (a)-(c) shows the qualitative results of the pre-possessing scheme adopted in this work. In order to segment the finger vein sample Fv from the background, we trace each column of Fv to determine the outer edge of the finger using the method described in [11]. This process will identify both upper and lower boundary of the finger vein Fv as illustrated in the Figure 8 (b). In the next step, we determine the central axis (or finger axis) Fv_a of the Fv by computing the midpoint between upper and lower boundary. We then estimate the rotation and translation parameters based on the obtained Fv_a by comparing it to the image reference axis [3]. Finally, affine image transform is employed to align the finger as shown in the Figure 8 (c). Finally, we obtain the ROI region that essentially represent the inner finger vein region by excluding the outer boundaries. To this extent, we first identify the tip of the finger vein TFv_a corresponding to the aligned finger vein sample by tracing its rows to find the first discontinuity [11]. In the next step, we increment the detected fingertip point TFv_a by X pixels along horizontal axis towards the end of the finger vein to obtain the new point $T\hat{F}v_a$. Now starting from this point $T\hat{F}v_a$, we define an area with Y pixels along vertical axis and L pixels along horizontal axis to obtain the ROI of the finger vein image Fv. The value of X,Y and L are determined on the development database and evaluated on the testing database. Figure 8 (d) shows the extracted ROI of the finger vein samples captured using our proposed scheme.

4.1.2 ROI extraction for fingerprint images

Figure 9 shows the pre-processing and ROI extraction for the fingerprint sample captured using our newly developed device. The pre-processing steps adopted for fingerprint samples will follow the similar step that we employed with finger vein images. Here, also we determine the bound-
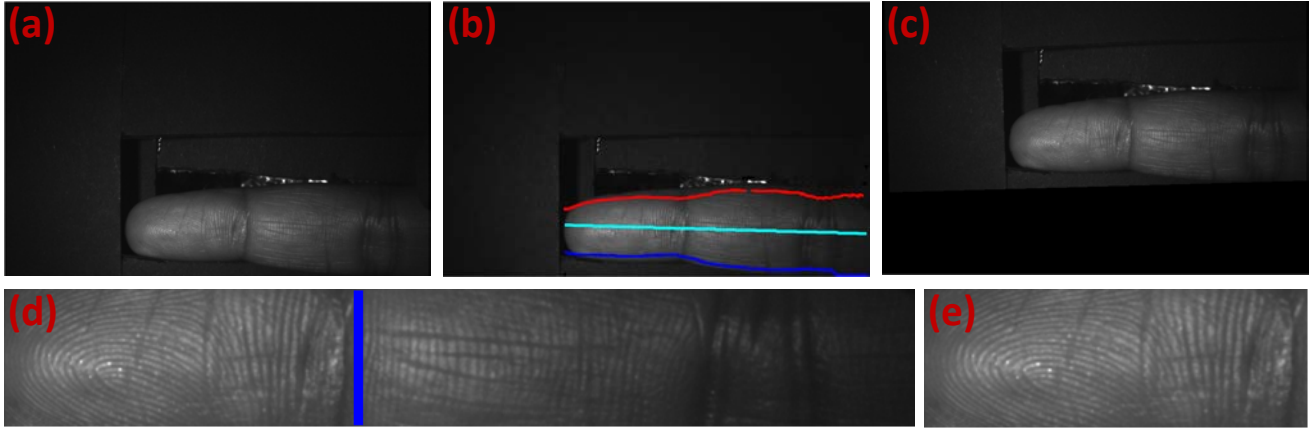
Figure 9. Illustration of fingerprint pre-processing and ROI extraction (a) Fingerprint sample (b) Boundary extraction (c) Alignment (d) Finger segmentation (e) ROI extraction

ary of the finger using the same method that we employed with finger vein. We then segment the finger by tracing the determined boundary points and then we obtain the finger axis by computing the midpoint between upper and lower boundary of the finger which in turn is used to align the finger by compensating for translation and rotation error. Figure 9 (b) shows the qualitative results of our pre-processing scheme to locate the boundary while Figure 9 (c) shows the aligned finger image. In the next step, we locate the tip of the aligned finger and finally segment the fingerprint part from the rest of the finger by analyzing the variation on local minima in the small region selected along the finger axis [11]. Figure 9 (d) shows the qualitative results of the estimated fingerprint boundary line (in blue color) to segment the fingerprint from the second phalanx of the finger and Figure 9 (e) shows the final fingerprint ROI submitted to the feature extraction component.

4.2. Feature extraction

Given the ROI of fingerprint sample, we first extract the minutiae locations using the NIST open source MINDTCT function [13] owing to the popularity and robustness for contact-less finger print recognition [11]. In this work, we employed the Spectral Minutiae Representation (SMR) [14] as the feature extraction scheme that can be effectively applied on both fingerprint and finger vein samples captured using our device. We made this choice by considering similar characteristics of finger vein and fingerprint especially in terms of minutiae pattern. Further, the use SMR feature extraction scheme will result in a fixed length feature vector, which is invariant to rotation, translation and scaling. There exits two variants of spectral minutiae representation schemes, namely: (1) Location based (2) Orientation based. In this work, we employed the location based SMR scheme by considering its improved performance especially on the finger vein biometrics [2].
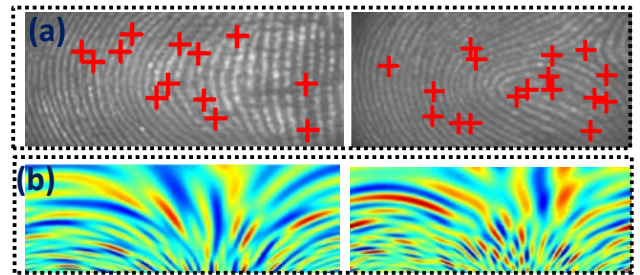

Figure 10. Illustration of qualitative results of SMR on fingerprint (a) Fingerprint samples (b) Real valued spectrum of SMR

4.2.1 Fingerprint feature extraction

The extracted minutiae location obtained using NIST open source MINDTCT function [13] is used to determine the SMR as suggested in [14]. Figure 10 (b) shows the qualitative results of the SMR on the fingerprint samples shown in the Figure 10 (a).

4.2.2 Finger vein feature extraction

For processing of finger vein images we propose a feature extraction based on the combination of the maximum curvature method and SMR. The proposed method differs from the state-of-the-art scheme mentioned in [2] by replacing its multi-scale filter method with the maximum curvature method [7] to accurately extract the finger vein pattern. Given the ROI of the finger vein sample as shown in the Figure 11 (a), we first perform the image enhancement using adaptive histogram equalization [15] as shown in the Figure 11 (b). We then use the maximum curvature method [7] to extract the connected vein pattern from the finger vein ROI. Figure 11 (c) shows the maximum curvature extracted from the enhanced image of Figure 11 (b). In the next step, we determine the minutiae points in the vein based on the
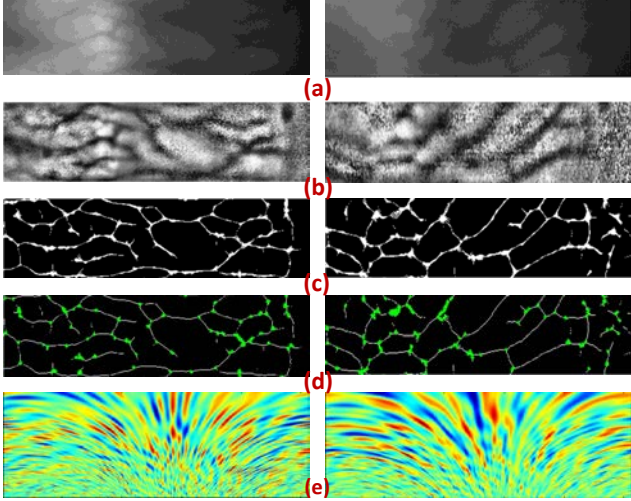
Figure 11. Illustration SMR on finger vein (a) finger vein samples (b) Image enhancement (c) Extracting maximum curvature pattern (d) Extracting minutiae points (e) Real valued spectrum of SMR

convolution filters [9] as illustrated in the Figure 11 (d). Finally, we use the location of the estimated minutiae points to compute the SMR as illustrated in the Figure 11 (e). The significance of our proposed finger vein recognition scheme over four different state-of-the-art schemes [7, 2, 6, 4] will be discussed in the Section 5. Note that the dimension of the SMR of both finger vein and fingerprint is of same dimension which is 128×256.

4.3. Comparison

In this work, we employed the cross-correlation [2] based comparator to obtain the similarity scores. Let $R(m, n)$ and $P(m, n)$ be the spectral minutiae representation of the reference and probe sample corresponding to the fingerprint (or a finger vein). We first normalize both $R(m, n)$ and $P(m, n)$ to have zero mean and unit variance. We then compute the similarity score S using normalized cross-correlation as follows:

$$S = \frac{1}{MN} \sum_{m,n} R(m, n)T(m, n) \qquad (1)$$

4.4. Weighted comparison score level fusion

Given the probe sample $P_{fp}(m, n)$ and $P_{fv}(m, n)$ that represent the fingerprint and finger vein respectively. We obtain the corresponding similarity scores S_{fp} and S_{fv} independently for fingerprint and finger vein respectively. We finally combine these similarity scores using the weighted sum rule [12] as follows:

$$F_{sc} = W_1 S_{fp} + W_2 S_{fv} \qquad (2)$$

Where, W_1 and W_2 indicates the weights on fingerprint and finger vein respectively such that $W_1 + W_2 = 1$ and F_{sc} denotes the fused score. In this work, we compute the weights

based on the individual performance [12]. The weights are calculated and optimized on the development dataset that in turn is used on the testing dataset to report the final performance.

5. Results and Discussion

This section will present the results on the multimodal biometric database comprised of fingerprint and finger vein captured using our sensor as described in the Section 2. The overall performance of the multimodal biometric system is presented in terms of Equal Error Rates (EER). Thus, the lower the value of EER the better is the system performance.

Table1 shows the performance of both unimodal and multimodal algorithms. The performance of the proposed finger vein recognition algorithm is benchmarked with the well-established four different state-of-the-art schemes based on the maximum curvature method [7], Spectral Minutiae Representation [2], Repeated line tracking method [6] and Gabor enhancement scheme [4].

Table 1. Performance achieved on our database captured using our proposed sensor

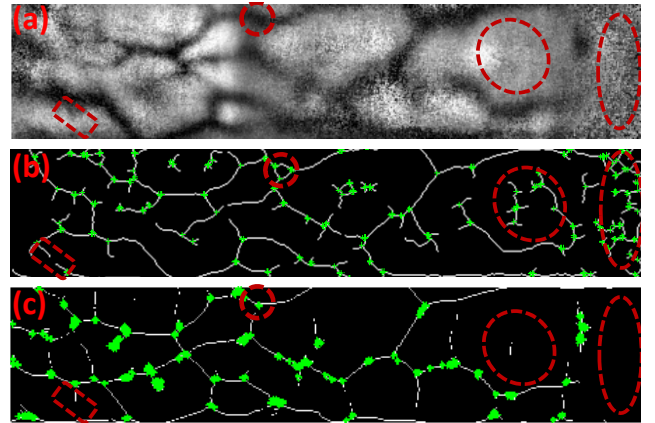| Modality	Algorithms	EER(%)
Finger vein	Repeated line tracking[6]	7.86
	Gabor enhancement [4]	12.45
	Maximum Curvature [7]	2.21
	SMR [2]	3.47
	Proposed Scheme	**1.74**
Fingerprint	MINDTCT with SMR [14]	6.83
Fusion	Weighted Sum rule	**0.78**

Figure 12. Qualitative evaluation of vein pattern extraction (a) Enhanced vein image (b) multi-scale filters adopted in [2] (c) maximum curvature adopted in this work

As observed from the Table1 the proposed scheme for finger vein has shown the best performance with EER = 1.74% when compared with four different state-of-the-art

schemes. Further, in order to visualize the possible reason for the improved performance of the proposed scheme when compared with [2], we illustrate the qualitative results of the multi-scale filters used in the state-of-the-art-scheme [2] (see Figure 12 (b)) and the maximum curvature method used in the presented work (see Figure 12 (c)) before extracting the vein bifurcation points and SMR. It can be observed from Figure 12 that the application of the maximum curvature method has various advantages since the use of multi-scale filters is not only computationally expensive but also very sensitive to the acquisition noise that will result in false vein patterns. This further justifies the robustness of the proposed finger vein scheme.

Table 1 also shows the quantitative performance of the captured fingerprint that also indicates the acceptable performance with EER = 6.63%. Finally, the score level fusion is carried using the weighted sum rule further improves the performance of the overall system with an EER = 0.78%. Note that, the comparison score level fusion result reported in this work employs the proposed finger vein scheme and fingerprint scheme as mentioned in the Section 4.2.2 and 4.2.1 respectively. The obtained results show the applicability of the proposed multimodal biometric sensor for real-life scenario.

6. Conclusion

We introduced a new multimodal biometric sensor that can simultaneously capture both fingerprint and finger vein samples. The proposed sensor is not only user friendly but it can also capture high quality fingerprint and finger vein samples so that one can extract prominent information useful for identity verification. We then collected a new multimodal biometric database comprised of 1500 fingerprint and finger vein corresponding to 150 fingers from 41 subjects. We also present the companion protocols to benchmark the performance of the state-of-the-art schemes. In addition to this, we also proposed the new scheme for finger vein recognition using maximum curvature and spectral minutiae representation. Extensive experiments carried out on our database indicate the superior performance of our proposed finger vein recognition scheme when compared with four well known state-of-the-art schemes. Finally, the comparison score level fusion of fingerprint and finger vein shows the best performance with EER = 0.78% that further justifies the applicability of both proposed sensor as well as proposed finger vein recognition algorithm for the real-life scenarios.

References

[1] O. Carnal and J. Mlynek. Young's double-slit experiment with atoms: A simple atom interferometer. *Physical review letters*, 66(21):2689, 1991.

[2] D. Hartung, M. Aastrup Olsen, H. Xu, H. Thanh Nguyen, and C. Busch. Comprehensive analysis of spectral minu-

tiae for vein pattern recognition. *IET Biometrics*, 1(1):25–36, March 2012.

[3] B. Huang, Y. Dai, R. Li, D. Tang, and W. Li. Finger-vein authentication based on wide line detector and pattern normalization. In *20th International Conference on Pattern Recognition*, pages 1269–1272, 2010.

[4] A. Kumar and Y. Zhou. Human identification using finger images. *IEEE Transactions on Image Processing*, 21(4):2228–2244, 2012.

[5] H. C. Lee, K. R. Park, B. J. Kang, and S.-J. Park. A new mobile multimodal biometric device integrating finger vein and fingerprint recognition. In *4th International Conference on Ubiquitous Information Technologies Applications*, pages 1–4, Dec 2009.

[6] N. Miura, A. Nagasaka, and T. Miyatake. Feature extraction of finger-vein patterns based on repeated line tracking and its application to personal identification. *Machine Vision and Applications*, 15(4):194–203, 2004.

[7] N. Miura, A. Nagasaka, and T. Miyatake. Extraction of finger-vein patterns using maximum curvature points in image profiles. *IEICE TRANSACTIONS on Information and Systems*, 90(8):1185–1194, 2007.

[8] Morpho. Think excellence, choose multimodality.

[9] M. Olsen, D. Hartung, C. Busch, and R. Larsen. Convolution approach for feature detection in topological skeletons obtained from vascular patterns. In *Computational Intelligence in Biometrics and Identity Management (CIBIM), 2011 IEEE Workshop on*, pages 163–167, April 2011.

[10] Y. H. Park, D. N. Tien, E. C. Lee, K. R. Park, E. C. Lee, S. M. Kim, and H. C. Kim. A multimodal biometric recognition of touched fingerprint and finger-vein. In *International Conference on Multimedia and Signal Processing*, volume 1, pages 247–250, May 2011.

[11] R. Raghavendra, C. Busch, and B. Yang. Scaling-robust fingerprint verification with smartphone camera in real-life scenarios. In *IEEE Sixth International Conference on Biometrics: Theory, Applications and Systems (BTAS)*, pages 1–8, Sept 2013.

[12] R. Raghavendra, H. Kumar, and A. Rao. Qualitative weight assignment for multimodal biometric fusion. In *2009 Seventh International Conference on Advances in Pattern Recognition*, pages 193–196, 2009.

[13] C. I. Watson, M. D. Garris, E. Tabassi, C. L. Wilson, R. M. Mccabe, S. Janet, and K. Ko. User's guide to nist biometric image software (nbis). 2007.

[14] H. Xu, R. Veldhuis, A. Bazen, T. A. M. Kevenaar, T. Akkermans, and B. Gokberk. Fingerprint verification using spectral minutiae representations. *IEEE Transactions on Information Forensics and Security*, 4(3):397–409, Sept 2009.

[15] K. Zuiderveld. Contrast limited adaptive histogram equalization. In *Graphics gems IV*, pages 474–485. Academic Press Professional, Inc., 1994.